Separation Microfluidic Devices Fabricated by Different Milling Processes

Inês M. Gonçalves[1,2], Miguel Madureira, Inês Miranda[3], Helmut Schütte[4], Ana S. Moita[2,5][a], Graça Minas[3], Stefan Gassmann[4] and Rui Lima[1,6]

[1]*METRICS, University of Minho, Guimarães, Portugal*
[2]*IN+, Instituto Superior Téncico, Universidade de Lisboa, Lisboa, Portugal*
[3]*Center for MicroElectromechanical Systems (CMEMS-UMinho), University of Minho, Guimarães, Portugal*
[4]*Jade University of Applied Science, Wilhelmshaven, Germany*
[5]*CINAMIL, Departamento de Ciências Exatas e de Engenharia, Academia Militar, Instituto Universitário Militar, Lisboa, Portugal*
[6]*CEFT, Faculty of Engineering of the University of Porto, Porto, Portugal*

Keywords: Separation Methods, Blood, Microfluidic Biomedical Devices, Micromilling.

Abstract: The diagnostic of several diseases can be performed by analysing the blood plasma of the patient. Despite of the extensive research work, there is still the need to improve the current low-cost fabrication techniques and devices for the separation of the plasma from the blood cells. Microfluidic biomedical devices have great potential for that process. Hence, two microfluidic devices made by micromilling and sealed with or without the solvent bonding technique were tested by means of a blood analogue fluid. A high-speed video microscopy system was used for the visualization and acquisition of the analogue fluid flow. Then, the separation of particles and plasma was evaluated using the software ImageJ. The device manufactured by the micromilling process without bonding showed a significant reduction of the amount of cells between the entrance and the exit of the microchannels. However, further analysis and optimizations of the microfluidic devices will be conducted in future work.

1 INTRODUCTION

Several diseases can affect the components of the blood, altering its rheological properties. Consequently, blood plasma and cells are commonly used for disease diagnosis and therapeutics (Yin *et al.*, 2013; Nam *et al.*, 2015; Shamloo *et al.*, 2016). Different information can be obtained from different components. For instance, the blood plasma is used to evaluate the inflammatory response and in proteomic studies, while the red blood cells are used to diagnose certain diseases (Lee *et al.*, 2014). Therefore, cell separation is important in medicine and performed millions of times per day over the world (Al-Fandi *et al.*, 2011; Bento *et al.*, 2019, Catarino *et al.*, 2019; Pinho et al. 2020). Nevertheless, some limitations still hinder the separation process. The most common techniques used are filtration and centrifugation. The former was the earliest to be used but has the disadvantage of filter clogging that leads to a reduction of the process efficiency (Lee *et al.*, 2014). Centrifugation is the most common method to separate blood cells from plasma and makes use of the density difference between the plasma and the cellular components (Nam *et al.*, 2019). One of the problems that arise from this technique is the cell damage due to the high shear forces which can lead to cell lysis and contamination of the plasma (Geng *et al.*, 2013). Developments in the field of microfluidics allowed the improvement of blood separation techniques with the fabrication of smaller devices with precise geometries, making the technology suitable for automation, low-cost, portable, with improved sterility and requiring less preparation time and amount of sample and reagents (Bento *et al.*, 2019, Nam *et al.*, 2019; Tsutsui and Ho, 2009; Ookawara *et al.*, 2010).

[a] http://orcid.org/0000-0001-9801-7617

Gonçalves, I., Madureira, M., Miranda, I., Schütte, H., Moita, A., Minas, G., Gassmann, S. and Lima, R.
Separation Microfluidic Devices Fabricated by Different Milling Processes.
DOI: 10.5220/0010906500003123
In *Proceedings of the 15th International Joint Conference on Biomedical Engineering Systems and Technologies (BIOSTEC 2022) - Volume 1: BIODEVICES*, pages 185-190
ISBN: 978-989-758-552-4; ISSN: 2184-4305

The design of the microfluidic devices has been developed to better mimic the geometry of in vivo microvascular networks. Different separation mechanisms were also developed and can be divided in active or passive methods (Dominical *et al.* 2015; Shamloo *et al.*, 2016). In the active methods, an external force is applied to move the cells apart from the plasma. Those forces can be gravitational, acoustic, magnetic, optical, chemical, electronic or electrical. The gravitational method is the most popular but has some limitations in microfluidic devices due to the interface tension, low Reynolds number and laminar flow that occur in flows at those dimensions (Xue *et al.*, 2012). On the other hand, passive techniques do not require an external force and are preferred to the active techniques due to ease of use and fabrication (Lee *et al.*, 2011; Nam *et al.*, 2015, Catarino *et al.*, 2019). The passive techniques depend on hydrodynamic effects that occur in the fluid when flowing through capillaries. If the Reynolds number is in values of unity order, the viscous forces balance the inertial forces and the red blood cells have the tendency to move towards the center of the channel, leaving a cell free layer (CFL) near the walls (Shamloo *et al.*, 2016). This phenomenon leads to the reduction of the apparent viscosity, a phenomenon called the Fåhræus-Lindqvist effect, and to less hematocrit in small vessels than in large ones (Yin *et al.*, 2013, Losserand *et al.*, 2019; Medhi *et al.*, 2019). The geometrical designs used for this type of microchannels include channel constriction, bending channel and bifurcated channels. Bending channels make use of centrifugal forces, constrictions in channels force particles to the center of the channel while bifurcations make use of the Zweifach–Fung effect. This effect consists in the tendency of the cells to travel to the branch channel of an asymmetric bifurcation with the higher flow rate since the pressure is lower (Fekete, *et al.*, 2012; Xue *et al.*, 2012; Meyari *et al.*, 2020).

In this work a microfluidic device for separation of cells and plasma was investigated. The device was composed of a microchannel with a series of three bifurcations and was fabricated by two different methods. Two blood analogues were used to infer on the efficiency of the cell clearance and the results were analysed using ImageJ software. Though further optimization of the design and fabrication process is still required, a significant reduction of cells was obtained with one of the microchannels.

2 MATERIALS AND METHODS

2.1 Microchannel Geometry

The proposed geometry was selected and optimized by taking into account several previous flow experiments performed by Lopes *et al.*, 2015, Singhal *et al.*, 2016 and Madureira *et al.*, 2018. Hence, the proposed microfluidic device is composed by four microchannels with the same geometry, but different depths. The microchannels comprise three separation segments connected in sequence. After the entrance the channel width narrows to force the cells to the center of the channel. Then, an intersection was placed so the cells continue forward to the exit while the plasma flows upward or downward through branch channels. Those channels that will merge again to form the main channel and the structure are repeated two more times. A scheme of the microchannel can be seen in Figure 1and the depth of each channel is presented in Table 1.

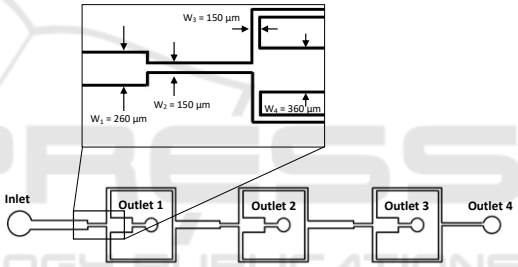

Figure 1: Microchannel geometry with detail showing the dimensions of the different regions of the segments.

Table 1: Depth of the different microchannels of the microfluidic devices.

		Microchannel	
		1 and 2	3 and 4
Manufacture 1	W_1, W_2, W_4	300 µm	150 µm
	W_3	100 µm	50 µm
Manufacture 2	W_1, W_2, W_4	300 µm	150 µm
	W_3	150 µm	50 µm

2.2 Fabrication Methods

2.2.1 Manufacture Process 1

One of the microfluidic devices was fabricated from poly(methyl methacrylate) (PMMA) through a micromilling process. The geometry of the microchannels was outlined using a CAD software and then the device was manufactured using a micromilling machine (Minitech Mini-Mill/GX. Two different micromilling tools were used for the manufacture, one with 100 μm and the other with 1 mm in diameter. The geometry was converted to NC code using the software Visual Mill so it could be read by the milling machine. Also, several parameters, such as, the angle, depth and velocity of the tool, were defined using that software. All the parameters were set to each of the used tools considering their different properties. Starting the milling process, the reference for the z-axis has to be set manually since the milling equipment has no height control. A magnifying camera was used to observe the first touch of the milling tool on the material. To avoid the damaging the milling tools due to the heat resulting from the high rotation speed, the work piece and the tools were cooled with a mixture of water and detergent during the milling process. More details of the micromilling process can be found elsewhere (Lopes *et al.*, 2015; Singhal *et al.*, 2016; Madureira *et al.*, 2018).

2.2.2 Manufacture Process 2

The second microchannel device was also manufactured by the micromilling technique above described. However, for this device, two PMMA plates were milled and then bonded together using the solvent bonding technique. The microchannels were milled in one plate and the other plate worked as the lid. After the milling and washing, the plates were placed together and exposed to a solvent vapor which creates an irreversible bonding between them. In the end of the treatment, the plates were pressed to ensure the bonding was maintained.
On both devices, stainless steel tubes with a length of about 1 cm and an inner diameter of about 1 mm were used as inlets and outlets of the microchannels. The tubes were fixed to the Plexiglass (acrylic glass, Plexiglas XT 0A000) using epoxy glue. The microchannel devices were then cleaned with water and detergent for 20 minutes using ultrasonication. Lastly, the devices were dried with pressurized air and sealed with an adhesive foil for PCR plates (Polyester 50 μm ultra-clear, non-sterile, heat-resistant).

2.3 Experimental Set-up

Flow visualization was performed using an inverted microscope (IX71, Olympus, Japan) and a high-speed camera (Fastcam SA3, Photron, USA). The microchannels were placed on the microscope connected to a syringe pump (CetoniNEMESYS Syringe Pump) to control the fluid flow. The experimental apparatus is presented in Figure 2.

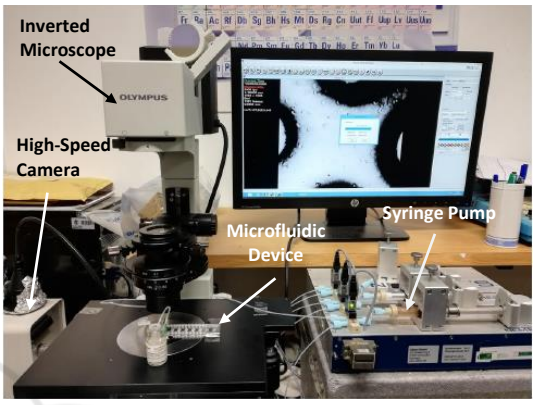

Figure 2: Experimental set-up used to perform the experimental microfluidic high-speed video recordings.

Two blood analogue solutions were made by adding the surfactant Brij L4 to distilled water at a concentration of 1 wt.%, as presented in (Lima *et al.*, 2020). The emulsion suspended phase is composed by spherical micelles with sizes ranging between 10 and 20μm. One of the solutions (Analogue 1) was then filtered by two filters of 10 and 20 μm average pore size while the other solution (Analogue 2) was just filtered with the 20 μm filter. Consequently, the fluids present spherical micelles with size ranging from 10 to 20 μm. Initially three different fluid flows, 60 μL/min, 100 μL/min and 150 μL/min, were compared and 100 μL/min was set for the remaining experiments.

2.4 Image Processing

The images from the microscope were obtained using a high-speed camera using a frame rate of 2000 and 6000 frames/second. The image sequences obtained were analysed using the minimum intensity feature of the Z-Project from the ImageJ software (Abràmoff *et al.*, 2004, Carvalho et al. 2021). The intensity of the pixels of a selected region was then evaluated and converted to a grey scale using the plot profile feature. High values correspond to brighter pixels which indicate regions with less particle density while lower values correspond to darker pixels and, consequently, high particle density or channel walls.

The grey value was measured transversely to the entrance and exit of the channel, using the Plot Profile feature of ImageJ. The average of the values obtained was then calculated and normalized, considering the maximum grey value obtained using water, to a scale of 0 to 1 for result comparison.

3 RESULTS AND DISCUSSION

The grey value was measured for the microchannel made by the first manufacture process using the Analogue 1 at three different fluid flows. Preliminary tests show that a greater variation between the entry and the exit is noted for 100 µL/min. The variation is similar for the other two flows, being lower for 60 µL/min (Figure 3).

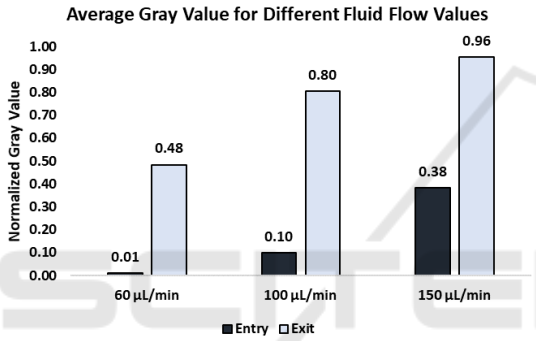

Figure 3: Variation of average grey value at the entrance and exit of the microchannel for different fluid flows.

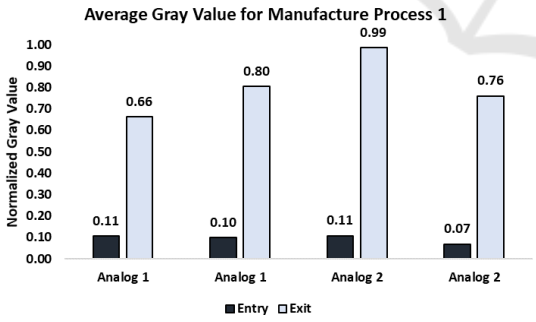

Figure 4: Variation of average grey value at the entrance and exit of the microchannel for manufacture process 1 at a 100 µL/min fluid flow.

Subsequently, the grey value variation was measured using both analogue fluids for the microchannel of the manufacture process 1 (Figure 4), and of the manufacture process 2, (Figure 5). The variation of the grey value between the entry and exit on both the microchannels was similar between the analogues. For the first manufacture process the variation was higher using the analogue 2, while for the second process the variation was higher with Analogue 1.

The influence of the depth of the microchannel was also investigated. The variation of the grey intensity on the different microchannels of the devices of manufacture 1 and 2 is presented in Figures 6 and 7, respectively. In the case of the former, the microchannels with lower depths showed higher clearance of cells while in the later the contrary was verified. Consequently, the tested deepness of the microchannels do not have a significant impact on the cell and plasma separation.

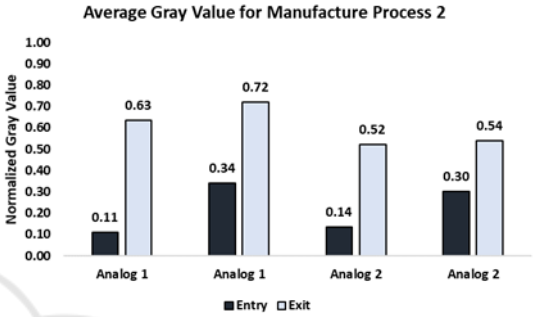

Figure 5: Variation of average grey value at the entrance and exit of the microchannel for manufacture process 2 at a 100 µL/min fluid flow.

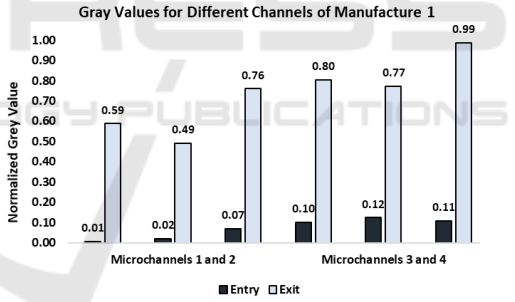

Figure 6: Variation of average grey value at the entrance and exit of the different microchannels of manufacture process 1 at a 100 µL/min fluid flow.

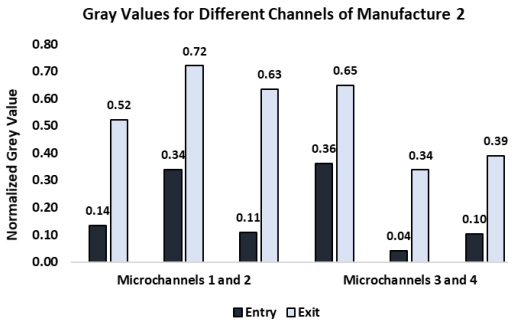

Figure 7: Variation of average grey value at the entrance and exit of the different microchannels of manufacture process 2 at a 100 µL/min fluid flow.

As expected, the grey value increased from the entry to the exit, indicating a reduction of the particle concentration throughout the microchannels. Difference in particle size does not seem to affect the clearance process since the results were similar using both of the analogue fluids. On the other hand, the fluid flow affects the efficiency of the microchannel. For first manufacture process it was possible to obtain high grey values corresponding to a reduction of the particle concentration. The grey values were also near the value obtained with water indicating a successful separation of the particles and plasma. Nevertheless, the detection is dependent on the resolution of the acquired images. Consequently, the minimum value, corresponding to the maximum amount of particles, obtained in each measurement varied. Further techniques and models for image acquisition and data treatment need to be improved for a better evaluation of the effectiveness of the device.

4 CONCLUSIONS

The present study shows the potentiality of a novel geometry for a microfluidic device for the separation of blood cells and plasma. The separation of the microparticles from the base fluid was mainly due to the successive contractions effect, where the particles tend to migrate into the center whereas the base fluid tend to flow towards the walls of the microchannel. From the two manufacture processes tested, the micromilling process without bonding showed promising results with grey values close to the ones obtained with water. The depth of the channels and the size of the particles did not show a major influence on the separation process. On the other hand, the fluid flow affected the results obtained, being 100 µL/min the flow that presented better results. Further image analysis studies and optimization of the geometry to improve the separation process will be performed in the near future.

ACKNOWLEDGEMENTS

Authors acknowledge FCT – Fundação para a Ciência e a Tecnologia for partially supporting this work through projects UIDB/00319/2020, UIDB/04077/2020, UIDB/00690/2020, UIDB/04436/2020 and PTDC/EME-SIS/30171/2017 NORTE-01-0145-FEDER-030171, and NORTE-01-0145-FEDER-029394 funded by COMPETE2020, NORTE 2020, PORTUGAL 2020, Lisb@2020 and FEDER and for supporting the PhD Fellowship (2020.08646.BD).

REFERENCES

Faustino, V.; Rodrigues, R.O.; Pinho, D.; Costa, E.; Santos-Silva, A.; Miranda, V.; Amaral, J.S.; Lima, R. A (2019), Microfluidic Deformability Assessment of Pathological Red Blood Cells Flowing in a Hyperbolic Converging Microchannel. *Micromachines*, *10*, 645.

Yin, X., Thomas, T., Zhang, J. (2013) Multiple red blood cell flows through microvascular bifurcations: Cell free layer, cell trajectory, and hematocrit separation. *Microvasc. Res.*, 89:47–56.

Shamloo, A., Vatankhah, P., Bijarchi, M.A. (2016) Numerical optimization and inverse study of a microfluidic device for blood plasma separation. *Eur. J. Mech. B/Fluids*, 57: 31–39.

Nam, J., Namgung, B., Lim, C.T., Bae, J.E., Leo, H.L., Cho, K.S., Kim, S. (2015) Microfluidic device for sheathless particle focusing and separation using a viscoelastic fluid. *J. Chromatogr. A*, 1406:244–250.

Lee, M.G., Shin, J.H., Choi, S., Park, J.K. (2014) Enhanced blood plasma separation by modulation of inertial lift force. *Sensors Actuators, B Chem.*, 190:311–317.

Al-Fandi, M., Al-Rousan, M., Jaradat, M.A.K., Al-Ebbini, L. (2011) New design for the separation of microorganisms using microfluidic deterministic lateral displacement. *Robot. Comput. Integr. Manuf.*, 27:237–244.

Bento, D., Fernandes, C.S. Miranda, J.M., Lima, R. (2019) In vitro blood flow visualizations and cell-free layer (CFL) measurements in a microchannel network. *Exp. Therm. Fluid Sci.*, 109:109847.

Catarino, S. O., R. O. Rodrigues, D. Pinho, J. M. Miranda, G. Minas, R. Lima. (2019) Blood Cells Separation and Sorting Techniques of Passive Microfluidic Devices: From Fabrication to Applications. *Micromachines*, 10, 593.

Pinho D, Carvalho V, Gonçalves IM, Teixeira S, Lima R. (2020) Visualization and Measurements of Blood Cells Flowing in Microfluidic Systems and Blood Rheology: A Personalized Medicine Perspective *Journal of Personalized Medicine* 10, 4, 249.

Nam, J., Yoon, J., Kim, J., Jang, W.S., Lim, C.S. (2019) Continuous erythrocyte removal and leukocyte separation from whole blood based on viscoelastic cell focusing and the margination phenomenon. *J. Chromatogr. A*, 1595:230–239.

Geng, Z., Ju, Y., Wang, W., Li, Z. (2013) Continuous blood separation utilizing spiral filtration microchannel with gradually varied width and micro-pillar array. *Sensors Actuators, B Chem.*, 180:122–129.

Tsutsui, H., Ho, C.M. (2009) Cell separation by non-inertial force fields in microfluidic systems. *Mech. Res. Commun.*, 36:92–103.

Ookawara, S., Oozeki, N., Ogawa, K., Löb, P., Hessel, V. (2010) Process intensification of particle separation by

lift force in arc microchannel with bifurcation. *Chem. Eng. Process. Process Intensif.*, 49:697–703.

Dominical, V.M., Vital, D.M., O'Dowd, F., Saad, S.T.O., Costa, F.F., Conran, N. (2015) In vitro microfluidic model for the study of vaso-occlusive processes. *Exp. Hematol.*, 43: 223–228.

Xue, X., Patel, M.K., Kersaudy-Kerhoas, M., Desmulliez, M.P.Y., Bailey, C., Topham, D. (2012) Analysis of fluid separation in microfluidic T-channels. *Appl. Math. Model.*, 36:743–755.

Lee, M.G., Choi, S., Park, J.K. Inertial separation in a contraction-expansion array microchannel. *J. Chromatogr. A*, 1218:4138–4143.

Losserand, S., Coupier, G., Podgorski, T. (2019) Migration velocity of red blood cells in microchannels. *Microvasc. Res.*, 124:30–36.

Lima, R.; Vega, E.J.; Moita, A.S.; Miranda, J.M.; Pinho, D.; Moreira, A.L.N. (2020) Fast, flexible and low-cost multiphase blood analogue for biomedical and energy applications. *Experiments in Fluids*, *61*, 231, doi:10.1007/s00348-020-03066-7.

Medhi, B.J., Reddy, M.M., Singh, A. (2019) Particle migration of concentrated suspension flow in bifurcating channels. *Adv. Powder Technol.*, 30:1897–1909.

Fekete, Z., Nagy, P., Huszka, G., Tolner, F., Pongrácz, A., Fürjes, P. (2012) Performance characterization of micromachined particle separation system based on Zweifach-Fung effect. *Sensors Actuators, B Chem.*, 162:89–94.

Meyari, M., Salehi, Z., Zarghami, R., Saeedipour, M. (2020) Numerical investigation of particle separation in Y-shaped bifurcating microchannels. *Particuology*, Corpus ID: 228863362

Lopes R., Rodrigues R. O., Pinho D., Garcia, V., Schutte H., Lima R., Gassmann S., (2015). Low cost microfluidic device for partial cell separation: micromilling approach. in Proceedings of 2015 IEEE International Conference on Industrial Technology, Seville, Spain.

Singhal, J., Pinho, D., Lopes, R., Sousa, P., Garcia, V., Schütte, H., Lima, R., Gassmann, S. (2016) Blood Flow Visualization and Measurements in Microfluidic Devices Fabricated by a Micromilling Technique. *Micro Nanosyst*, 7:148–153.

Madureira, M., Faustino, V., Schütte, H., Gassmann, S., Lima, R. (2018) Blood cells separation in a T-shaped microchannel fabricated by a micromilling technique. *J. Mech. Eng. Biomech.*, 2:43–49.

Abràmoff, M.D., Magalhães, P.J., Ram, S.J. (2004) Image processing with imageJ. *Biophotonics Int.*, 11:36–41.

Carvalho, V.; Gonçalves, I.M.; Souza, A.; Souza, M.S.; Bento, D.; Ribeiro, J.E.; Lima, R.; Pinho, D. (2021) Manual and Automatic Image Analysis Segmentation Methods for Blood Flow Studies in Microchannels. *Micromachines*, *12*, 317.